International Journal of Fatigue 206 (2026) 109459

Contents lists available at ScienceDirect

International Journal of Fatigue

journal homepage: www.elsevier.com/locate/ijfatigue

Analytical and machine learning-based fatigue life prediction of welded joints under multiaxial loading☆

Marten Beiler [a], Niklas Michael Bauer [b], Jörg Baumgartner [b], Moritz Braun [a,c,*]

[a] German Aerospace Center (DLR), Institute of Maritime Energy Systems, Geesthacht, Germany
[b] Fraunhofer LBF, Fraunhofer Institute for Structural Durability and System Reliability, Darmstadt, Germany
[c] Hamburg University of Technology, Institute of Ship Structural Design and Analysis, Hamburg, Germany

ARTICLE INFO

Keywords:
Fatigue strength assessment
Multiaxial fatigue
Artificial neural network
Extreme gradient boosting
Explainable AI
SHAP analysis

ABSTRACT

Evaluating the fatigue life of welded joints under multiaxial loading is a key challenge in structural engineering. This study explores machine learning (ML) methods for predicting fatigue life and compares their performance against the novel super ellipse criterion, which is an analytical approach that aims to improve current design standard methods (e.g., Eurocode 3, IIW). Using a dataset of uniaxial and multiaxial fatigue tests with varying phase angles, ML models—including artificial neural networks and extreme gradient boosting (XGBoost)—are trained on features like stress amplitudes, phase differences, and material properties. Artificial neural networks provide high accuracy, while tree-based models like XGBoost offer better interpretability via model agnostic interpretation using Explainable Artificial Intelligence. Results show ML models can outperform traditional criteria, especially under non-proportional loading, but face limitations near the edges of the training data. This work highlights the potential and challenges of ML in fatigue prediction and highlights their value for enhancing the safety and reliability of welded structures.

1. Introduction

Fatigue life evaluation of welded joints under multiaxial loading presents a significant challenge in structural engineering, requiring accurate prediction methods to ensure safety and reliability. Herein, multiaxial fatigue loading in welded joints refers to the simultaneous action of different types of stresses—most commonly, normal stresses (σ_x) acting perpendicular to the weld and shear stresses (τ_{xy}) acting parallel to it. This combination creates a complex stress state that significantly influences fatigue behavior and makes accurate fatigue assessment challenging.

Two primary types of multiaxial loading conditions are typically considered: proportional and non-proportional loading. In proportional loading, the stress components vary over time but maintain a constant phase relationship ($\sigma_x(t)/\tau_{xy}(t) = \text{const.}$). As a result, the directions of the principal stresses remain fixed, and the loading scenario can often be approximated by uniaxial loading applied at an inclined angle to the weld [1]. Consequently, traditional assessment methods may still yield reasonable predictions in such cases; however, in non-proportional loading, the stress components vary independently and are out of phase with one another ($\sigma_x(t)/\tau_{xy}(t) \neq \text{const.}$), have different stress ratios ($R_\sigma \neq R_\tau$), or have different frequencies ($f_\sigma \neq f_\tau$). This leads to a time-dependent rotation of the principal stress directions, introducing additional complexity into the fatigue process. Experimental studies have shown that such conditions can lead to increased fatigue damage [2], and the mechanisms governing fatigue crack initiation [3] and growth may differ significantly from those under proportional or uniaxial loading [4], which is addressed in design standards by higher safety factors.

To address these complexities, a wide range of multiaxial fatigue criteria have been developed and proposed in the literature. These criteria generally fall into four broad categories: stress-based interaction equations, equivalent stresses, critical plane approaches, and integral approaches. Stress-based interaction methods attempt to combine the effects of normal and shear stresses using mathematical formulations, while critical plane models focus on evaluating stresses and strains on specific material planes where fatigue damage is most likely to initiate. Integral approaches are based not only on the most critical plane but integrate an equivalent stress over all planes.

Despite many years of research on multiaxial fatigue, there is still no

☆ This article is part of a special issue entitled: 'ICMFF14' published in International Journal of Fatigue.

* Corresponding author at: German Aerospace Center (DLR), Institute of Maritime Energy Systems, Geesthacht, Germany.
E-mail address: moritz.braun@dlr.de (M. Braun).

https://doi.org/10.1016/j.ijfatigue.2025.109459
Received 1 October 2025; Received in revised form 28 November 2025; Accepted 23 December 2025
Available online 24 December 2025

general agreement—neither among design codes or within the research community—on a single, universally applicable multiaxial fatigue criterion for welded joints. The variability in experimental results, coupled with the diverse nature of multiaxial stress states, continues to pose a significant challenge in selecting and applying the most appropriate fatigue assessment model. As a result, engineers and researchers often rely on a combination of empirical data, theoretical frameworks, and engineering judgment when evaluating the fatigue performance of welded structures subjected to complex multiaxial loading.

ML methods offer a promising alternative to traditional—often either empirical or numerical—methods, as ML methods are particularly successful at capturing and modeling complex data interactions. The potential of ML has been demonstrated in numerous studies; nevertheless, significant differences exist between ML models. Traditional ML models, e.g., based on decision trees, are statistical in nature and focus on the identification of patterns within the data. On the other hand, artificial neural networks learn to approximate complex relationships in data by adjusting weights in a layered structure and by using nonlinear activation functions to capture both simple and complex patterns. Both approaches offer distinct advantages. Artificial neural networks, as purely black-box models, often achieve higher accuracy compared to traditional ML methods; however, models that leverage data patterns directly tend to be more interpretable, which enables reliable interpretation of results and to reveal hidden correlations within the data.

This study compares various ML approaches to a state-of-the-art design criterion, i.e., the super ellipse criterion [5], for assessing the fatigue life of welded joints. A comprehensive dataset comprising uniaxial fatigue test results under nominal and shear loading, as well as multiaxial fatigue test data with varying phase angles, forms the basis of the analysis. The ML models are trained to predict fatigue life using a diverse set of features derived from stress amplitudes, phase differences, and material properties. The super ellipse criterion [5], a novel analytical method, serves as a benchmark for evaluating ML performance.

This approach specifically seeks to analyze data interactions leading to the fatigue life predictions, compare the results to state-of-the art assessment, and assess the interpretability and effectiveness of these methods in providing insights into complex fatigue phenomena. Beyond neural networks, the study also employs the ensemble tree-based algorithm, Extreme Gradient Boosting (XGBoost), to predict fatigue life based on multiaxial fatigue test data from welded joints, with the resulting predictions being compared. To facilitate model-agnostic interpretation of the XGBoost predictions, the Shapley Additive Explanations (SHAP) framework is utilized. This work highlights the advantages and limitations of ML models for fatigue life prediction and provides insights into their application to enhance the reliability of welded structures subjected to multiaxial stresses. In addition, the results of the ML models are interpreted using partial dependence plots by assessing the relation between fatigue life a variation of selected input variables. This facilitates an assessment of the results based on domain knowledge.

2. Multiaxial fatigue of welded joints

Fatigue of welded joints under multiaxial loading is under investigation since around the 1960s for proportional loading and since around the 1980s for non-proportional loading [6]; however, even if multiaxial loading is quite common in cyclically loaded structures, available fatigue data is rare. Only around 20 experimental campaigns on welded steel joints have been published, which performed fatigue tests under non-proportional loading. In these investigation, sometimes only two fatigue tests have been performed for identical load scenarios [7]. Thus, the data basis is limited.

Nevertheless, various fatigue assessment approaches have been applied on the existing data and found introduction into common rules and guidelines, such as the IIW-recommendations [8], Eurocode 3 [9], DNV [10] or FKM [11]. The majority of guidelines use interaction equations for the assessment that takes into account the degree of utilization, i.e., the ratio between acting and endurable stresses. Despite the general similarities, the details of the approaches vary and lead to high differences in the resulting assessment. One example is the effect of non-proportionality: Whereas the IIW-recommendation proposes a reduction of fatigue strength by a reduction of a so-called comparison value, which can be interpreted as a penalty factor, the FKM-guideline provides different criteria for proportional and non-proportional loading. The Eurocode, however, does not consider this damaging effect, even so it is experimentally proven [2]. This shows, that there is still, after 50 years of research uncertainties on the influences of multiaxial and especially non-proportional stress states.

3. Analytical and machine learning-based fatigue life predictions for multiaxial fatigue tests

3.1. Super ellipse criterion

The super ellipse criterion (SEC) [12] is a multiaxial fatigue assessment criterion assuming ductile material behavior, i.e., a fatigue life reduction under non-proportional compared to proportional loading [13]. It has been developed on the basis of the presented database by optimization of its parameters and provides both accurate and precise predictions for all test programs included, while outperforming commonly used criteria from the literature and guidelines. Accordingly, it will serve as a benchmark for evaluation of the machine learning approaches based on the experimental nominal stresses.

Based on an interaction equation, the SEC assumes a super elliptical relationship between the cyclic degrees of utilization of both the stress range normal to the weld $\Delta\sigma_\perp$ and shear stress range $\Delta\tau$ for a given cycle number N under both proportional and non-proportional loading. The utilization describes the ratio between the applied stress to the endurable stress, denoted as the fatigue resistance $\Delta\sigma_{\perp_R}(N)$ and $\Delta\tau_R(N)$, which is derived from the corresponding uniaxial S-N curve for a given cycle number N. The SEC is presented in the following:

$$\left(\frac{\Delta\sigma_\perp}{\Delta\sigma_{\perp_R}(N)}\right)^c + \left(\frac{\Delta\tau}{\Delta\tau_R(N)}\right)^c \leq 1. \tag{1}$$

To predict fatigue life, the SEC is transformed into an equation and solved numerically with respect to N. Multiaxial loading is differentiated using an exponent of $c = 2.15$ for proportional and $c = 1.26$ for non-proportional loading. The super elliptical relationships of the utilizations inherent to Equation (1) are shown graphically in Fig. 1 for both proportional and non-proportional loading.

Within this publication, the SEC is evaluated based on fatigue

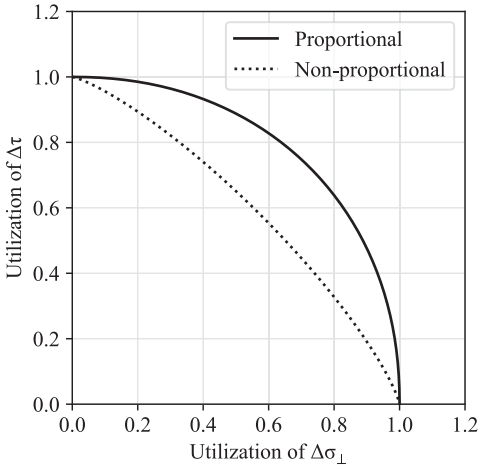

Fig. 1. Graphical illustration of the super ellipse criterion.

resistances derived directly from the corresponding experiments under uniaxial loading. The choice of the stress concept, i.e. the nominal, structural, notch, or effective stress concept, is therefore irrelevant, as the stress concentration factors would be applied to both the applied and the endurable stress range and thus cancel each other out; however, the application of the SEC can also be based on design S-N curves from codes or standards for any stress concept by determining the corresponding applied stress components within the given stress concept. An evaluation based on effective stresses derived by the critical distance and the stress averaging approach has shown good results [14].

3.2. Machine learning based methods

Machine learning techniques are data-driven methods that are created to yield accurate prediction in requiring tasks. In the context of fatigue assessment of welded joints, ML methodologies have shown significant promise, as they can process multivariate data swiftly and capture complex non-linear interactions among various parameters—such as load characteristics, geometrical features, and material properties. While ML models excel in computational efficiency and predictive accuracy, their successful implementation often requires large, high-quality datasets [15] and/or a solid incorporation of domain knowledge to evaluate and interpret results [16]. Interpretable models are essential, as they must allow experts to validate predictions against established mechanical principles. Moreover, the generalizability of ML models can be challenged if new data fall outside the feature space of the training dataset, leading to potential issues like overfitting and reduced reliability, see Barbiero et al. [17]. Consequently, the verification and validation of ML predictions become crucial before the deployment for fatigue life assessment. Such methods offer an attractive alternative to traditional fatigue assessment approaches that often rely on idealizations and simplifications.

There are plenty of studies on the applications of ML-based models to assess the fatigue strength of machined or additively manufactured components even under multiaxial loading [18]; however, studies on welded joints are limited.

Among various machine learning methods, artificial neural networks are most widely used for fatigue assessment [19]. Common input features for fatigue life prediction models include load- and material-related parameters, defect characteristics such as size and location, and stress concentration factors [20]. Recent approaches, aim to assess the fatigue strength of welded joints by including information about the weld geometry, c.f., [21–23]. This is, however, only possible if detailed information about the weld geometry, e.g., from optical surface scans are available. The data for the present study is taken from various studies and thus not contain such data. Thus, the assessment is limited to loading conditions, phase differences, and material properties, which is subsequently presented in more detail.

3.2.1. Artificial neural network

Fatigue assessment under multiaxial loading is one of the most challenging fields in structural engineering due to the complex interactions between stress and strain across different directions. Traditional deterministic models, such as critical plane or energy-based approaches, rely on simplified assumptions and material-specific empirical data. These methods often lack the flexibility needed to capture nonlinear effects and variability in real-world loading conditions.

Artificial neural networks (ANNs) provide a purely data-driven alternative by learning direct mappings between input features and fatigue-related outputs without presupposing functional forms. ANNs consist of input, hidden, and output layers where interconnected neurons apply nonlinear activation functions, enabling the network to capture complex relationships in experimental datasets. Their flexibility allows them to process diverse mechanical and loading parameters simultaneously, making them suitable for multiaxial fatigue applications [24].

Applications of ANNs in this context include fatigue life prediction and the estimation of missing material parameters essential for multiaxial criteria. For instance, ANNs have been used to predict fatigue life directly from experimental datasets under complex load paths, demonstrating improved accuracy compared with traditional empirical models. They have also been applied to estimate fatigue strengths (e.g., axial and torsional fatigue limits) when direct experimental data are unavailable, thereby enabling the application of multiaxial fatigue criteria [25]. In comparative studies, neural network models achieved prediction quality on par with or better than conventional regression and other machine learning techniques, although dataset size remains a critical factor in their performance [24,25].

3.2.2. Extreme gradient boosting

Another data-driven alternative to traditional methods is Extreme Gradient Boosting (XGBoost), which is an ensemble machine learning method that builds predictive models from multiple sequentially optimized regression trees. Unlike conventional regression, it excels at handling nonlinear relationships, variable interactions, and heterogeneous datasets, making it suitable for fatigue problems where stress states, material properties, and multiaxial loading histories interact in complex ways [25]. The method incorporates both boosting and regularization, which reduces overfitting and improves generalization even on relatively small experimental fatigue datasets.

The feature-importance functionality of XGBoost and the possibility to link it to model agnostic interpretation tools such as SHAP also allowed identification of the most influential mechanical and fatigue properties for parameter estimation, thereby enhancing interpretability of the predictions.

In multiaxial fatigue applications, XGBoost has rarely been used for fatigue life estimation, see, e.g., Zhang et al. [24]; however, it is more frequently used for fatigue assessment under uniaxial loading [21,26–30]. This is, however, not surprising given the few studies on fatigue life estimation under multiaxial loading in general.

4. Database on multiaxial fatigue tests of welded joints

The database consists of fatigue tests of welded joints under constant and variable amplitude pure normal stress, pure shear stress, proportional, and out-of-phase loading while showing ductile material behavior. All stresses are nominal stresses. To each multiaxial fatigue test there are corresponding fatigue test series under pure normal and shear stress with sufficient individual points to derive meaningful S-N curves. Other types of non-proportionality as well as stresses parallel to the weld are not considered due to the very limited number of tests in the literature. Runouts are excluded within the prediction of multiaxial fatigue life. Failure refers to through-thickness cracking or fracture. Table 1 and Fig. 2 provide a broad overview of each multiaxial fatigue test program and the corresponding characteristics. A test program is defined as all fatigue tests with equal uniaxial fatigue resistance.

The uniaxial reference stress-life (S-N) curves required for multiaxial fatigue assessment are derived from experiments, including runouts, using the maximum likelihood method by optimization in the direction of the fatigue life, while clamping failure has been interpreted as runout [13]. Knee points could be determined only for some tests sets based on aluminum and magnesium. For the remaining test sets and in accordance with the IIW recommendations [8], a knee point of 10^7 has been assumed for normal stresses and a knee point of 10^8 for shear stresses, both curves have a slope after the knee point of $m = 22$. Variable amplitude loading always refers to Gaussian distributions and is transformed to constant amplitude equivalents based on the S-N curve under constant amplitude loading according to the Palmgren-Miner rule as stated within the IIW recommendations [8]:

Table 1
Multiaxial fatigue database for welded joints with ductile material behavior (T-T: Tube-Tube, T-F: Tube-Flange, aw: as welded, sr: stress relieved, gr: ground flush, P: proportional, OOP: out-of-phase, *specimens from Razmjoo under pure torsion loading partially failed in the weld throat) [13].

#	Primary author(s)	Specimen	Material	Thickness in mm	Weld condition	Amplitude	R	Phase shift in °	Failure location	Number P/ OOP
01	Eibl [31]	T-T	Steel (St 35)	2	aw	constant	−1	90	Root	18/8
02	Exel [32]/ Bolchoun [33]	T-T	Magnesium (AZ31)	1.5	aw	constant/ variable	−1	45, 90/45	Root	18/19
03	Exel [32]/ Bolchoun [33]	T-T	Magnesium (AZ61)	1.5	aw	constant/ variable	−1	45, 90/45	Root	17/22
04	Bertini [34], Frendo [35]	T-F	Steel (S355JR)	10	aw	constant	−1	90	Root	10//9
05	Bertini [34], Frendo [35]	T-F	Steel (S355JR)	10	aw	constant	0	90	Root	11/8
06	Razmjoo [36]	T-F	Steel (BS 4360 Grade 50E)	3.2	aw	constant	0	90	Toe*	7/7
07	Sonsino [37]/ Sonsino [38]	T-F	Steel (StE 460)	10	sr	constant/ variable	−1	90	Toe	15/17
08	Sonsino [37]	T-T	Steel (StE 460)	6	sr + gf	constant	−1	90	Toe	9/9
09	Störzel [39]	T-T	Steel (S235 G2T)	1	aw	constant	−1	45, 90	Root	21/24
10	Wiebesiek [40]	T-T	Aluminum (AlMg3,5Mn)	1.5	aw	constant, variable	−1	45, 90	Root	27/31
11	Wiebesiek [40]	T-T	Aluminum (AlSi1MgMn T6)	1.5	aw	constant, variable	−1	45, 90	Root	23/19
12	Winther [41]	T-T	Steel (S355J2H)	3.1	aw	constant	−1	22.5, 45, 67.5, 90	Toe	5/25
13	Witt [42]	T-F	Steel (StE 460)	8.0	sr	constant, variable	−1	90	Toe	16/14
14	Witt [42]	T-F	Steel (StE 460)	8.0	sr	constant, variable	0	90	Toe	13/15

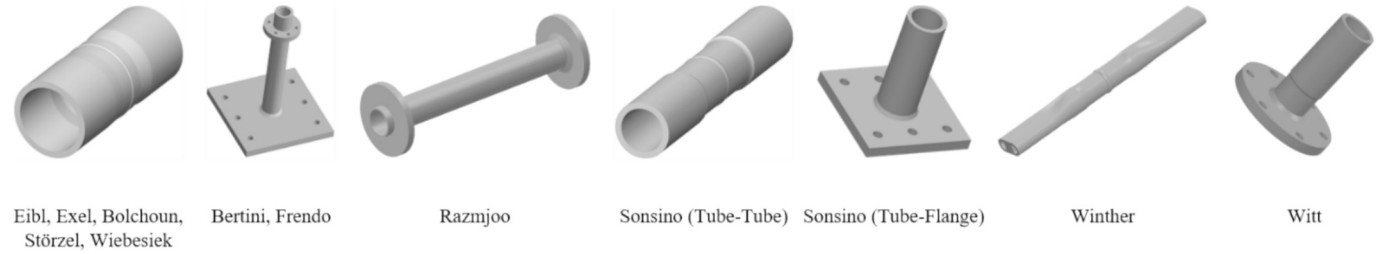

Fig. 2. Specimens from the database [13].

$$\Delta\sigma_{eq} = \sqrt[m_k]{\frac{1}{D_{spec}} \bullet \frac{\sum\left(n_i \bullet \Delta\sigma_i^{m_k}\right) + \Delta\sigma_{knee}^{m_k - m_l} \bullet \sum\left(n_j \bullet \Delta\sigma_j^{m_l}\right)}{\sum n_i + \sum n_j}} \tag{1}$$

while m denotes the slope of the S-N curve, n the number of cycles for each load spectrum block, and D_{spec} the specific Miner sum with $D_{spec} = 0.5$ under assumption of no high fluctuations of the mean stresses. The indices i and k refer to the values above the knee point, the indices j and l to those below the knee point of the S-N curve for $\Delta\sigma_{eq} \geq \Delta\sigma_{knee}$ or vice versa for $\Delta\sigma_{eq} < \Delta\sigma_{knee}$.

5. Results of analytical and machine learning-based fatigue assessments of multiaxial fatigue tests of welded joints

5.1. Super ellipse criterion

The relationship between the utilizations of $\Delta\sigma_{\perp}$ and $\Delta\tau$ is close to an elliptical relationship under proportional loading. The lower exponents under non-proportional loading reflect a less curvy correlation corresponding to a higher penalty for more similar utilizations of both stress components. This can be interpreted as a fatigue life reduction factor which depends on the ratio between both stress components. As opposed to methods with a constant penalty factor [8,10], the utilization automatically becomes 1 if the loading is uniaxial. Accordingly, no differentiation as to whether both stress components are significant enough to justify the penalty has to be made as this is implicitly and continuously considered. Based on the presented database, these relationships proved to describe the utilizations derived from the experiments under both proportional and non-proportional very well [13], even though the available number of fatigue tests with one dominant stress component is very limited. An extension by the stress component parallel to the weld is recommended with the same exponent, resulting in a super ellipsoid criteria, but validated yet only for proportional loading [5]. The predicted fatigue life over the true number of cycles from the multiaxial fatigue tests is shown in Fig. 3.

5.2. Artificial neural network

5.2.1. Prediction results

Artificial neural networks are trained on the basis of the presented database using k-fold cross-validation (CV) by differentiating between test programs to prevent overfitting. The implementation is based on the open source python library PyTorch (version 2.2). Program-wise cross validation is relevant as each test program is based on the same fatigue resistance and hence the same input variables for the ANN. Accordingly, for the fatigue life prediction of each of the 14 test programs, a neural network is trained based on the fatigue data of all the other test programs [13]. Random cross-validation without differentiation between test programs and varying ratios of training and test data resulted in a very similar prediction quality. To avoid any effect of variable amplitude loading, only constant amplitude loading is used for training.

The input parameters consist of the applied normal stress range $\Delta\sigma_{\perp}$,

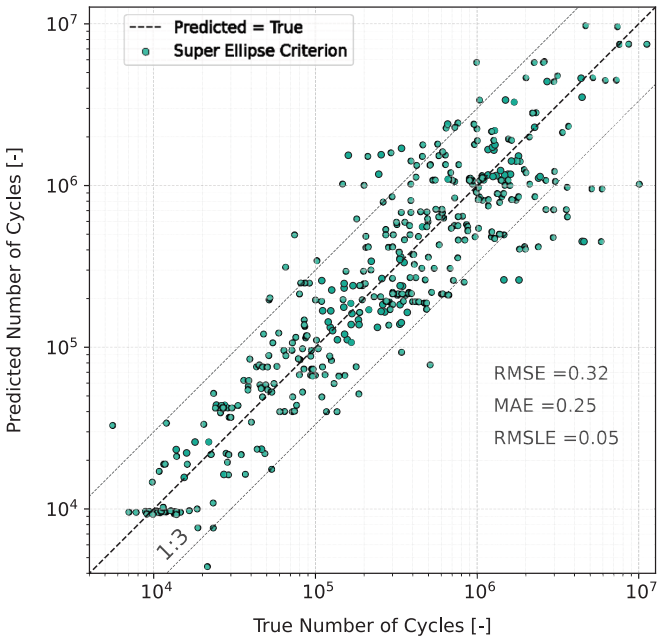

Fig. 3. Predicted number of cycles from the SEC over the true number of cycles from fatigue testing.

the shear stress range $\Delta\tau$, the phase shift, as well as the parameters of the fatigue resistance S-N curves under uniaxial loading $\Delta\sigma_{\perp_R}(N)$ and $\Delta\tau_R(N)$, i.e., the stress and cycle number at the knee point as well as the slopes before and after the knee point, neglecting the slope after the knee point for shear stress due to high correlations with the slope for normal stress. All input and output variables are transformed to logarithmic values to facilitate training by realizing similar magnitudes.

The ANN are constructed based on two hidden layers with 8 nodes each and a ReLU activation function, see Fig. 4. Training is performed using backpropagation while applying batch normalization to scale the inputs of all layers to similar means and variances. The issue of local minima is addressed using mini-batches (10 samples per batch), momentum (factor of 0.5), and multiple random weight initializations. Furthermore, as dropout did not enhance the training process, only regularization (factor of 0.5) is applied to avoid overfitting. Detailed information on the hyperparameter optimization are given in Table 2. The prediction results are shown in Fig. 5 where the predicted number of cycles from the ANN is plotted versus the true number of cycles from the fatigue tests.

5.2.2. Dependence plots

The results and behavior of the neural networks can be interpreted via partial dependence plots (PDP). Partial dependence plots are created by calculating the mean fatigue life over a variation of selected input

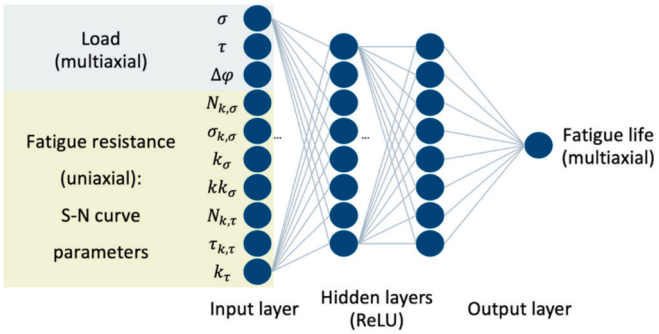

Fig. 4. Architecture of the artificial neural network.

Table 2
Hyperparameters of the artificial neural network [13].

Parameters	Value
Minibatch size	10
Momentum	0.5
Dropout	0.0
Regularization	0.5

variables within the test data while keeping all remaining variables constant. Since the variables relating to the uniaxial fatigue resistance are derived from experiments, load related variables such as the applied normal and shear stress are varied assuming a phase shift of 0°, 45°, and 90°. Fig. 6 shows an averaged partial dependence plot over all neural networks on a scalar and logarithmic scale.

The ANN learned a curved relationship between normal and shear stress for a given cycle number. Since the logarithmic applied stresses are used as input to the ANN, the logarithmic plot on the left directly shows the learned behavior of the ANN; however, a transformation to linear values allows a better interpretability. For areas with a dominant stress component, the presented relationship is not statistically supported as there is no corresponding data within the database. Also, high stress levels are based only on very few test programs with similar normal to shear stress ratios, while the lower and medium stress levels are based on various fatigue test programs with varying normal to shear stress ratios. Considering the statistically sound areas under multiaxial loading as well as uniaxial loading, a super elliptical relationship can be derived on both a logarithmic and a linear scale.

In the partial dependence plots, fatigue life increases with increasing stress in certain regions due to missing data in areas dominated by one stress component, making those regions unrepresentative. Both plots clearly show a significant reduction of endurable stresses, which is equivalent to a reduction in fatigue life, under out-of-phase loading compared to proportional loading. The fatigue life reduction seems to increase with a higher phase shift, as for most stress levels, a 45° phase shift reduces the endurable stresses by half as much as with a 90° phase shift. Moreover, the effect of phase shifts declines when one stress component becomes comparably small as the curvature under out-of-phase loading is less pronounced. The influence of the magnitude of each stress component cannot be clearly correlated with the effect of out-of-phase loading. To better understand the effect of stress levels in interaction with the phase shift, a partial dependence plot is created analogous to Fig. 6 by varying the phase shift along with each of both stress components while averaging the results over each fatigue test, i.e. for each experimental value of the other stress component, within the corresponding test program, see Fig. 7.

Fig. 7 shows a linear correlation between the phase shift and the endurable stress range for a given fatigue life for both stress components. An increase in each of both stress components leads to a similar and slightly increasing effect of phase shifts; however, the reduced effect at lower stress levels might be due to specimens made of aluminum and magnesium, as only they are subjected to stress ranges around 50 MPa and less. Moreover, since the underlying database includes almost exclusively phase shifts of 45° and 90°, the predictions between these values are not statistically justified, but interpolated.

The ratio of shear to normal stress is commonly assumed to influence the fatigue life under out-of-phase loading. As the combined effect of three variables on the fatigue life is not displayable anymore, the fatigue life reducing effect under 90° phase shifts compared to in-phase loading is investigated with respect to the corresponding shear to normal stress ratio directly using a fatigue life factor. The fatigue life factor for a given stress component ratio is defined as the average ratio of the predicted fatigue life under 90° phase shift to 0° phase shift over all corresponding fatigue tests. The resulting factors for each stress component ratio with sufficient fatigue tests to derive at least one S-N curve are shown in

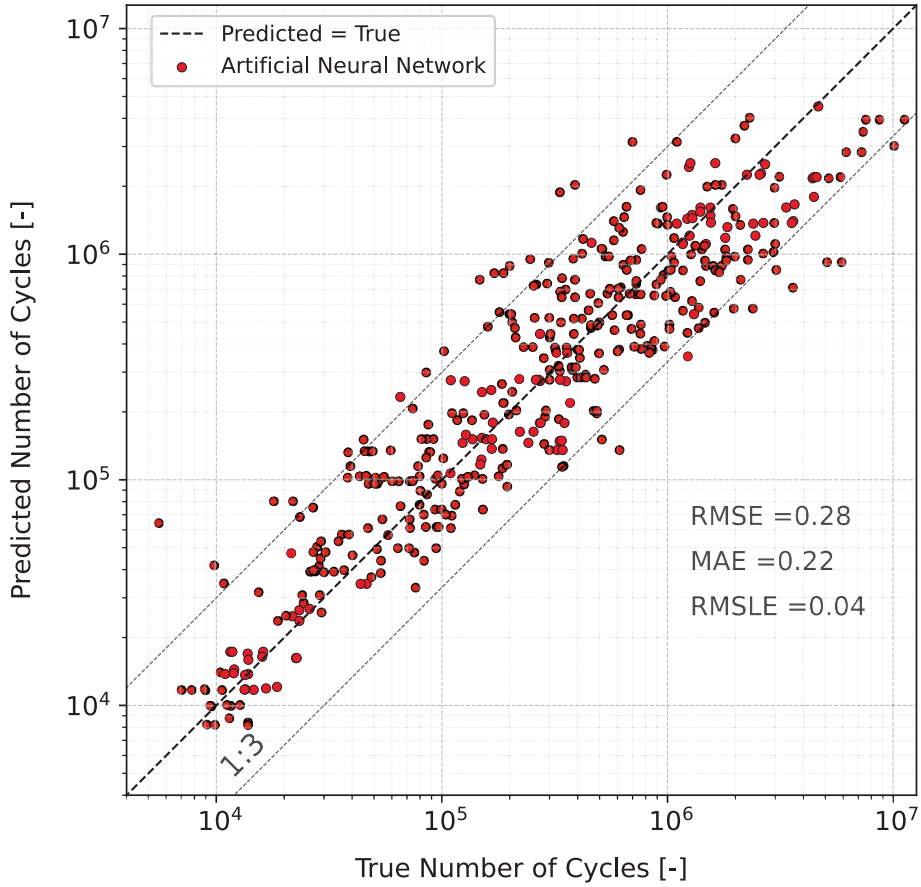

Fig. 5. Predicted number of cycles from the ANN over the true number of cycles from fatigue testing.

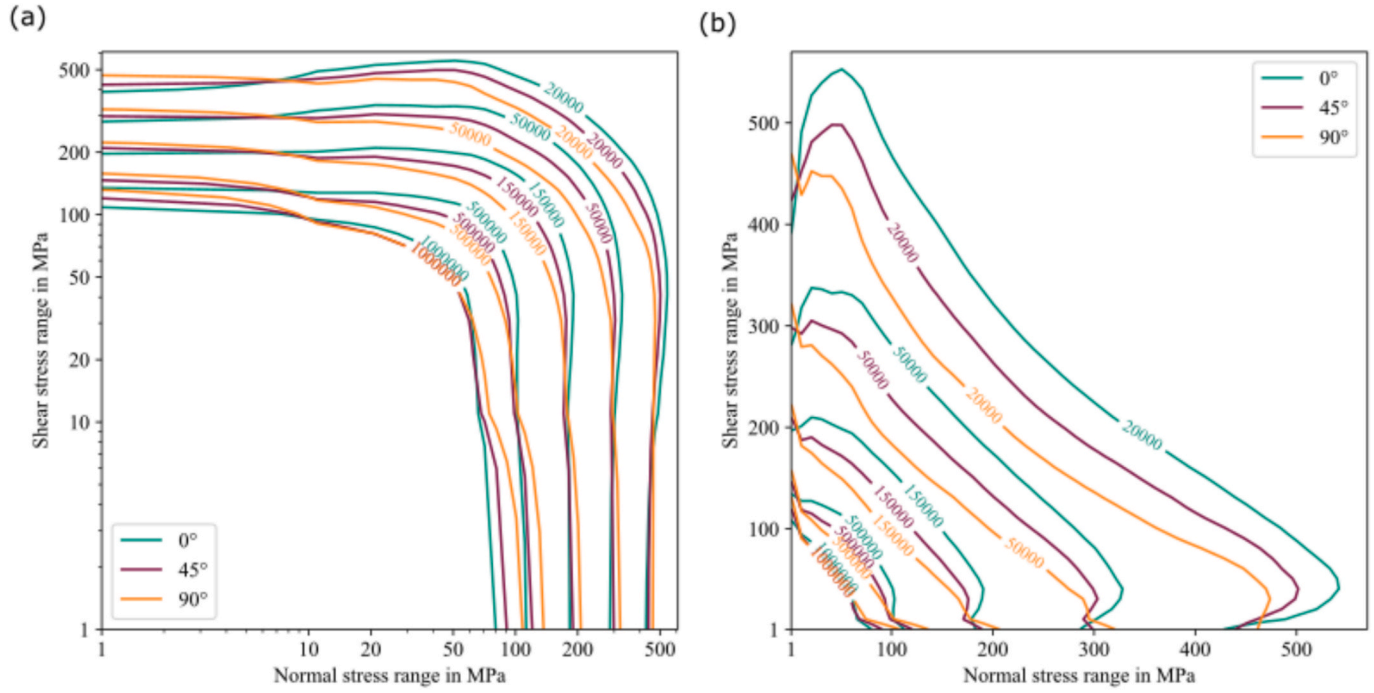

Fig. 6. Partial dependence plot on a logarithmic scale (a) and a linear scale (b).

Fig. 8.

The number of different stress component ratios is limited to the marked values; however, Fig. 8 indicates a higher effect of out-of-phase loading for similar stress levels. Since the fatigue resistance under shear loading is often higher than under normal loading, the highest effect is expected at a stress component ratio slightly above 1, corresponding to a

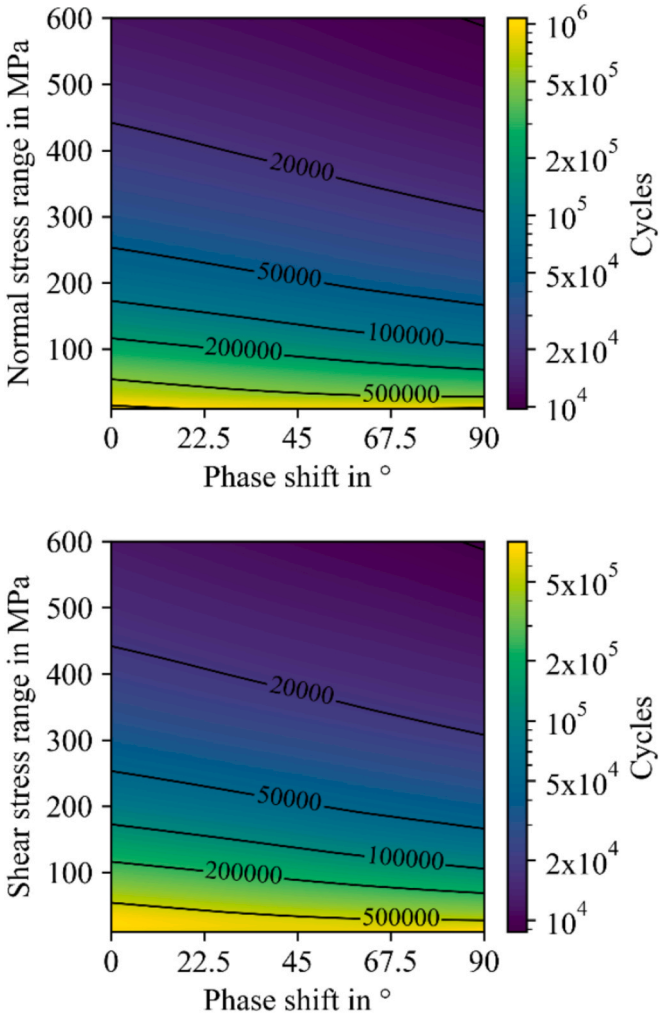

Fig. 7. Partial dependence plot on the influence of phase shifts.

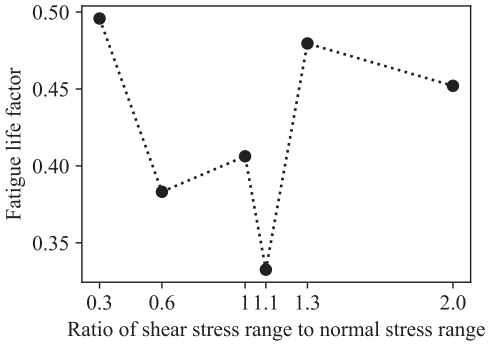

Fig. 8. Fatigue life reduction under 90° compared to 0° phase shift as a function of the ratio of shear to normal stress.

similar damaging effect of both stress components under uniaxial loading. Furthermore, Fig. 8 allows quantifying the effect of out-of-phase loading inherent in the ANN with a fatigue life reduction by around 50 %–70 %.

5.3. Extreme gradient boosting

Artificial neural networks seem well suited to estimate the fatigue strength under multiaxial loading, as they are able to approximate a continuous and piecewise linear functional representation of the semi-elliptical relationship describing the fatigue behavior of welded specimens under non-proportional loading, especially when using the ReLU activation function. In contrast, the XGboost-algorithm combines data sequentially using decision trees [13]. As a result, also an approximation of the physical relationship is learned based on the statistical data structures without explicitly mapping the underlying physical relationship; however, the approximation is not as smooth as the one of the ANN and offers a piecewise constant approximation [43]. This section analyzes the predictive performance of XGBoost across various feature configurations and prediction scenarios, comparing the results with those of the ANN and the SEC for forecasting the fatigue life of welded specimens under non-proportional loading. The XGBoost-model is built using the open source python library xgboost (version 2.1.1).

5.3.1. Predictions with stress-life curve parameters

The S-N curve parameters are specific to individual test programs and describe the fatigue strength under the respective test conditions. These parameters are utilized as features for the XGBoost-model together with the load-related parameters including interaction parameters like the phase shift between the normal and the shear stress. The analysis also distinguishes between a random split for the creation of the 14 CV folds and a program-wise split. While the random split highlights the model's predictive ability within the overall data domain, the program-wise split forces the model to make predictions for previously unseen data constellations. Fig. 9(a) shows the predicted number of cycles for the program-wise split and Fig. 9(b) for the random split. The random splitting for the CV demonstrates good prediction accuracy according to the applied error metrics which are even lower than metrics of the ANN and the SEC. On the other hand, the prediction accuracy for the program-wise splits is significantly lower for XGBoost.

An advantage of the XGBoost-framework is the interpretability of the tree structure. This allows analyzing the decision-making process retrospectively with, e.g., the SHAP-framework. SHAP is a game-theoretical framework for interpreting the predictions of machine learning models. For XGBoost, SHAP uses a model-specific TreeExplainer to efficiently compute the contribution of each feature to individual predictions [44]. This allows further investigations to be carried out in addition to the pure comparison of the predictions, such as analyzing the influence of S-N curve parameters on the prediction accuracy. The TreeExplainer is built using the open-source python library shap (version 0.45.1).

Fig. 9(c) shows the mean of the SHAP values for the prediction made by the randomly split 14-fold CV and the influence of the respective feature value on the SHAP values. The SHAP beeswarm plot on the right side of the figure visualizes the distribution of SHAP values for each feature, where each point represents an individual specimen. The horizontal position reflects the feature's contribution to the predicted fatigue life, and the color indicates the corresponding feature value. The most influential features in the model are the shear stress and normal stress, which aligns with theoretical expectations. Notably, positive SHAP values, which indicate an increase in the predicted fatigue life, are associated with low stress values. This implies that the model predicts longer fatigue life under lower applied stresses, which is consistent with physical understanding. The next most impactful features are the knee point and the scatter of the normal stress S-N curves. This highlights that S-N curve parameters have a significant influence on the fatigue life prediction in the XGBoost model. Moreover, the phase shift proves to be a crucial feature for the predictions, revealing a clear trend in its effect on the output. In the presence of a phase shift, the predicted number of cycles decrease and vice versa. In contrast, many of the features are found to have no significant impact on the predictions. For example, the stress ratios and the mean stresses barely affect the predictions. Similarly, the specimen type shows no significant influence.

5.3.2. Predictions separated by material classes

The previous analysis shows that the XGBoost model is able to

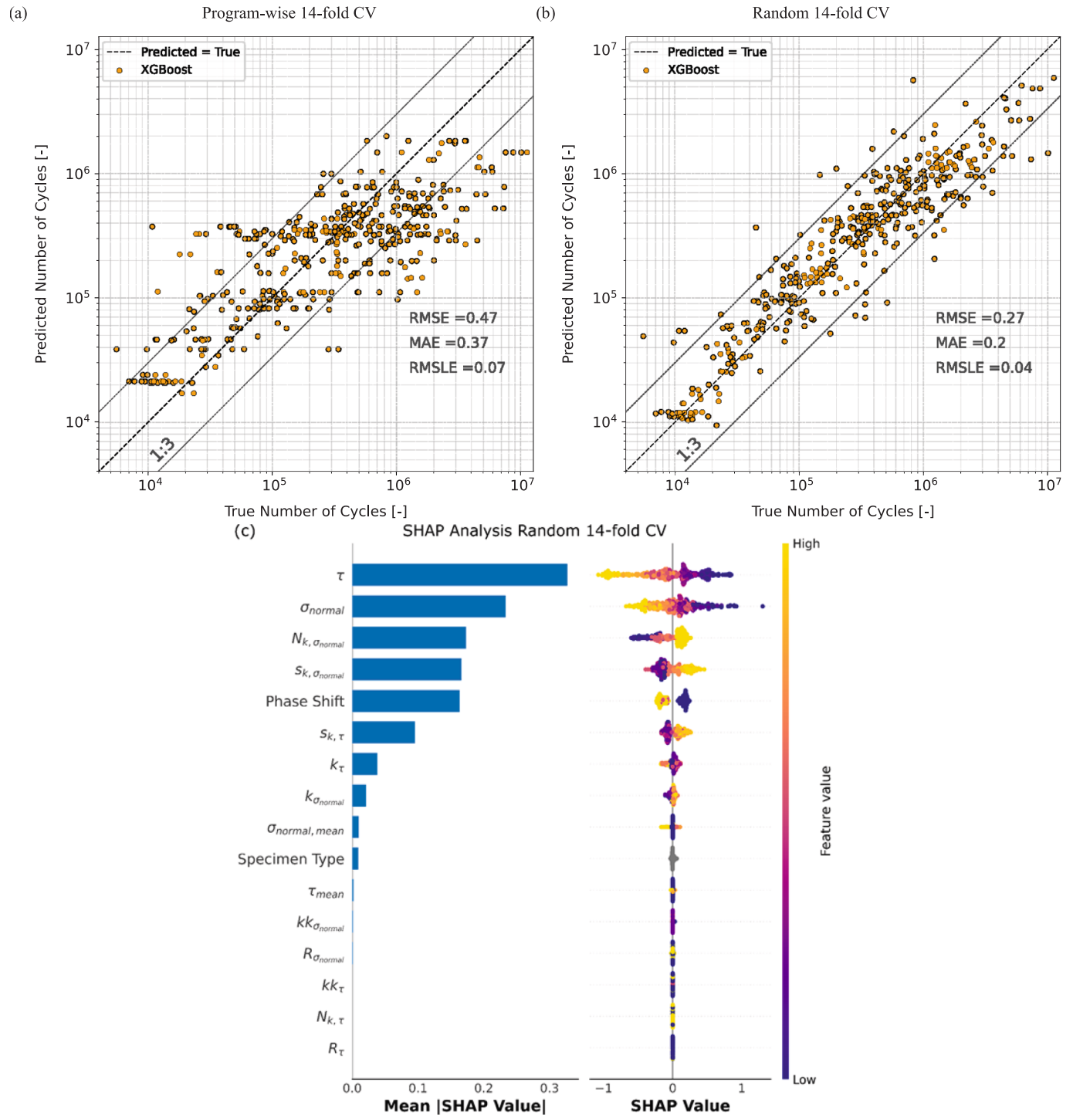

Fig. 9. The predicted number of cycles from program wise CV (a) and the predicted number of cycles from randomly shuffled 14-fold CV (b) with the XGBoost-Algorithm over the true number of cycles from the fatigue tests. SHAP Analysis of the predictions made by the random 14-fold CV (c).

reliably predict the fatigue strength when the data is randomly split. This is especially true when S-N curve parameters are included as features; however, if a program-wise CV is used, the model performance drops significantly. This indicates that the model strongly benefits from test program-wise information contained in the training set when randomly split.

In order to check the generalizability of the XGBoost model, the training is therefore restricted to features that cannot be clearly assigned to a single test program. By encoding categorical features such as material class or weld seam condition, further influencing variables can be included in the prediction. Instead of specific material designations, only superordinate material classes (aluminum, steel, magnesium) are used. This makes it possible to investigate whether the model can make generalizable predictions even without direct knowledge of program specific characteristics. It turns out that the prediction accuracy for a random CV (RMSE = 0.31) is slightly worse but still close to that of the ANN (RMSE = 0.28) (Fig. 10(a)). In contrast, the prediction accuracy remains at the same level with a program-wise split as when using the program-wise split with the S-N curve parameters. This shows that the model can identify generalizable relationships, but only within the

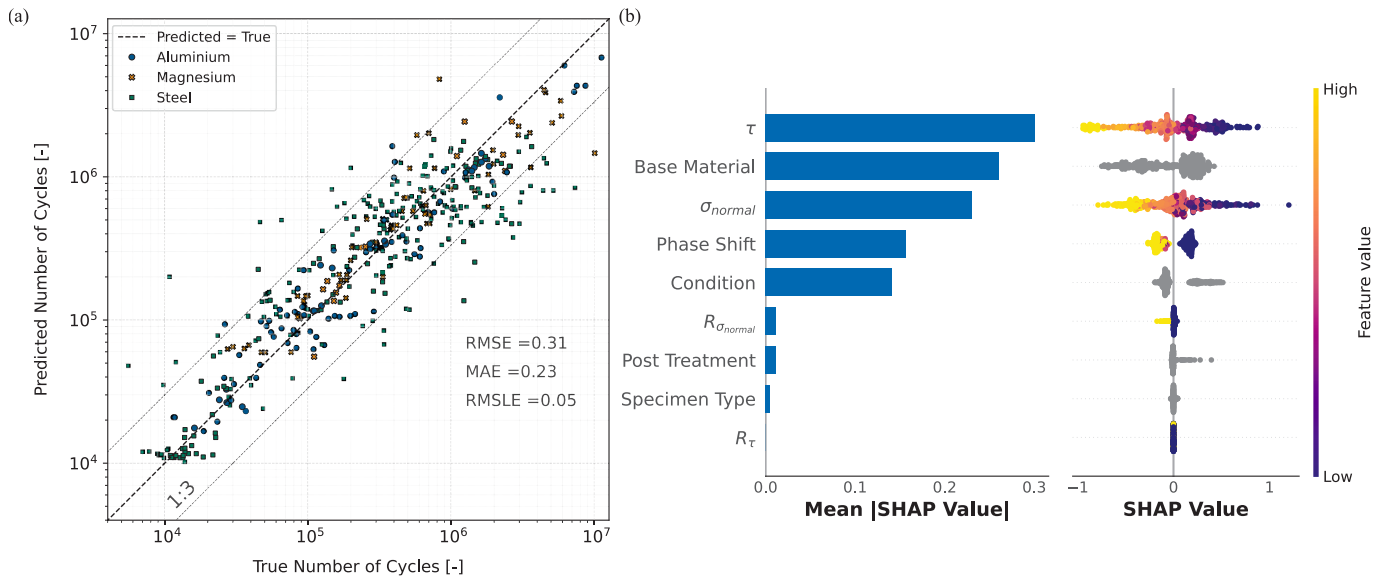

Fig. 10. Predicted number of cycles from randomly shuffled 14-fold cross-validation using program-spanning features with the XGBoost algorithm versus the true number of cycles from fatigue tests (a). SHAP analysis of the corresponding predictions (b).

programs, not across them.

Having a closer look on the materials in Fig. 10(a), one observes differences in the prediction accuracy for the respective materials. The specimens made of steel show a greater scatter of the predictions than the specimens with aluminum or magnesium as the base material. Additionally, the SHAP analysis in Fig. 10(b) shows a high influence of the base material on the fatigue life prediction. Feature values are not assigned in the SHAP beeswarm plot because the encoded categorical features do not represent actual values what results in grey points; however, also the weld condition (as-welded or stress relieved) has an impact on the XGBoost prediction while the post treatment (as-welded or ground flush) and the specimen type (tube-tube or tube-flange) do not play a role for the prediction.

5.3.3. Predictions without information about material and stress-life curve parameters

The analysis of the base material's influence has shown that it significantly affects fatigue strength prediction—comparable to the impact of the S-N curve parameters. While the S-N curve parameters can be directly attributed to individual test programs, the distribution of material classes spans multiple programs, offering broader generalization potential; however, this raises the question of whether such categorical features are essential at all. Both the SEC and ANN models achieve accurate predictions without relying on categorical inputs like material class. Consequently, the investigation of the XGBoost-based approach is extended to include predictions based solely on stress-related features, in order to assess the model's performance without categorical dependencies.

The prediction accuracy decreases slightly, while comparing Fig. 11 (a) with Fig. 10(a) and Fig. 9(b), for this feature constellation, but is still within the SEC range; however, it is noticeable that there are more outliers, some of which deviate significantly from the true value. The SHAP analysis shows that only four features actually contribute significantly to the model prediction—the shear stress, the normal stress, the

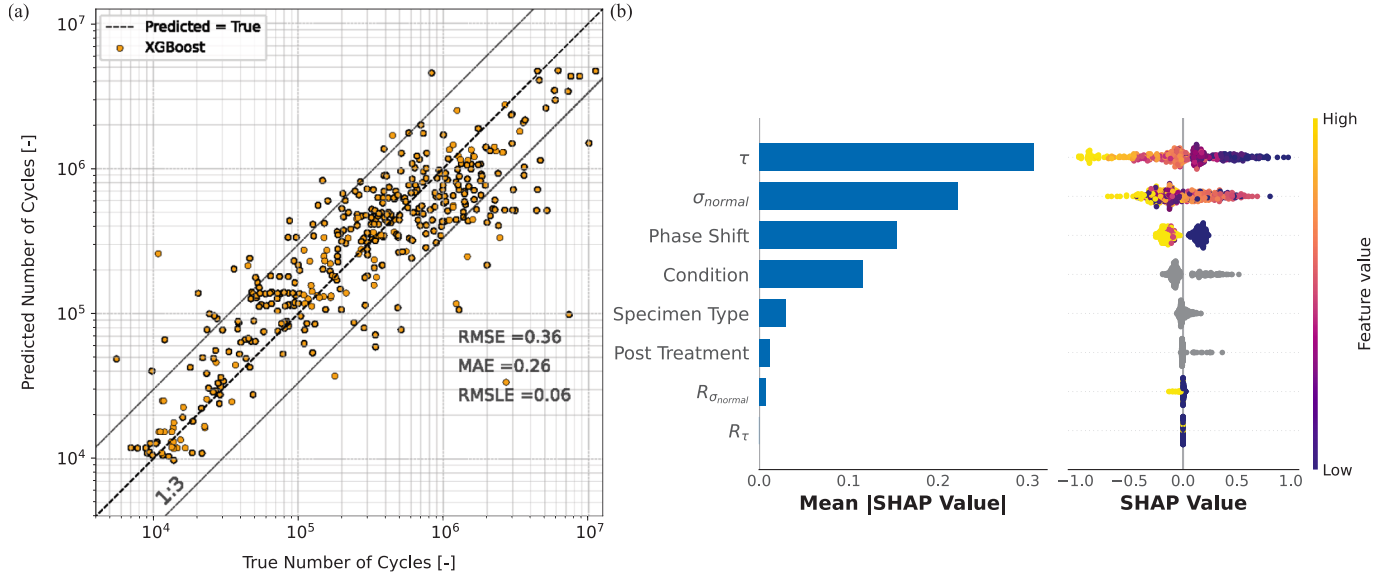

Fig. 11. Predicted number of cycles from randomly shuffled 14-fold cross-validation using only stress-related features with the XGBoost algorithm versus the true number of cycles from fatigue tests (a). SHAP analysis of the corresponding predictions (b).

phase shift and the weld seam condition. It is striking that the normal stress values cannot longer be assigned so clearly to the level of the SHAP values. Medium normal stresses are also associated with high SHAP values. In contrast, the influence of the shear stress and the phase shift on the model prediction remains almost unchanged.

5.3.4. Model agnostic interpretation

The differentiated analysis of the features has shown that certain parameters—such as the base material or specific S-N curve characteristics—can significantly influence the model's predictions. Nevertheless, the principal stress directions and their phase shift remain the most decisive factors in predicting fatigue life. As demonstrated with the ANN and implemented in the SEC approach, the semi-elliptical relationship between the principal stress components forms the basis for reliable fatigue life predictions. The partial dependence plot in Fig. 12 shows the influence of the stress directions on the fatigue life prediction for the XGBoost model trained on the stress-related features and the S-N curve parameter. For the comparison with the ANN the program-wise CV is chosen. The same semi-elliptical relationship between the stress components can also be found for the XGBoost model; however, it is noticeable that there are local deviations and the curves are less smooth. This observation is typical for tree-based models such as XGBoost. Due to the binary division of the feature space during training, discrete decision thresholds arise, which appear in the PDPs as abrupt jumps or plateaus. These locally sharp transitions can be an indication of limited generalizability in data-poor regions, as has been shown for the program-wise CV.

5.4. Comparison of results

Despite the different approaches, the fatigue life prediction using XGBoost also shows a good estimation of the fatigue strength as long as the training data domain covers the test splits. In case the test split is not covered by the training data domain, the poor extrapolation ability of the ensemble tree method becomes obvious. Since the XGBoost algorithm relies on stochastical data splits no physical relationships are learned. The difference is clearly shown by the comparison of the CV routines; the random split in 14 folds works much better than the test program wise splits. This can also be seen after features that can be directly associated with specific programs have been removed and partly replaced by program-spanning features. This indicates that the fatigue strength of the welds is strongly dependent on the respective test program, e.g., due to specific load types, test setups, geometries, etc., which cannot be adequately represented by general features; however, inside the training data domain the XGBoost model works well and performs similarly as the ANN. Fig. 13 directly compares the prediction accuracies using identical feature sets, including S–N curve parameters, showing the results of the 14-fold cross-validation with random splits for the XGBoost model and a program-by-program split for the ANN, whose performance is largely unaffected by the choice of data splitting strategy.

A comparison of the PDPs of ANN and XGBoost shows that a more constant relationship between the stress directions and the fatigue strength is learnt using ANN. With the XGBoost-model, it can be seen that the semi-elliptical relationship is only learnt selectively, particularly in the data-poor range. This indicates that more data is required for the XGBoost-model, which depicts more test programs, if the predictions are to be made for new test programs; however, if the database is diverse enough, the XGBoost-model works excellently, as has been shown in the CV with random split.

6. Discussion

The comparison of the extended classical approach with the SEC and the ML based fatigue life predictions shows that the ML based prediction has great potential for fatigue strength assessment of non-proportionally loaded welds. The complexity of the interaction of the different characteristics makes the usage of ML methods for this type of prediction particularly interesting, as they are generally better able to map nonlinear and high-dimensional relationships; however, the comparison between ANN and XGBoost shows that different ML algorithms have different characteristics with regard to the required features and

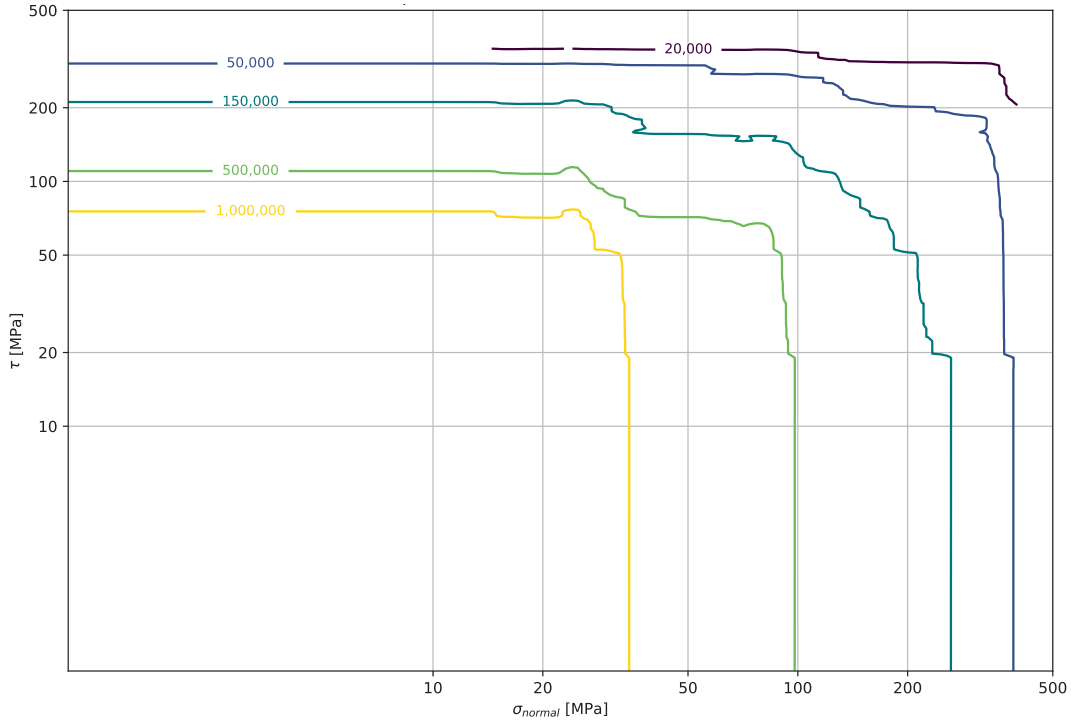

Fig. 12. Partial Dependence Plot showing the dependence of the shear stress and the normal stress on the fatigue life prediction for the XGBoost model on logarithmic scale for fixed prediction levels.

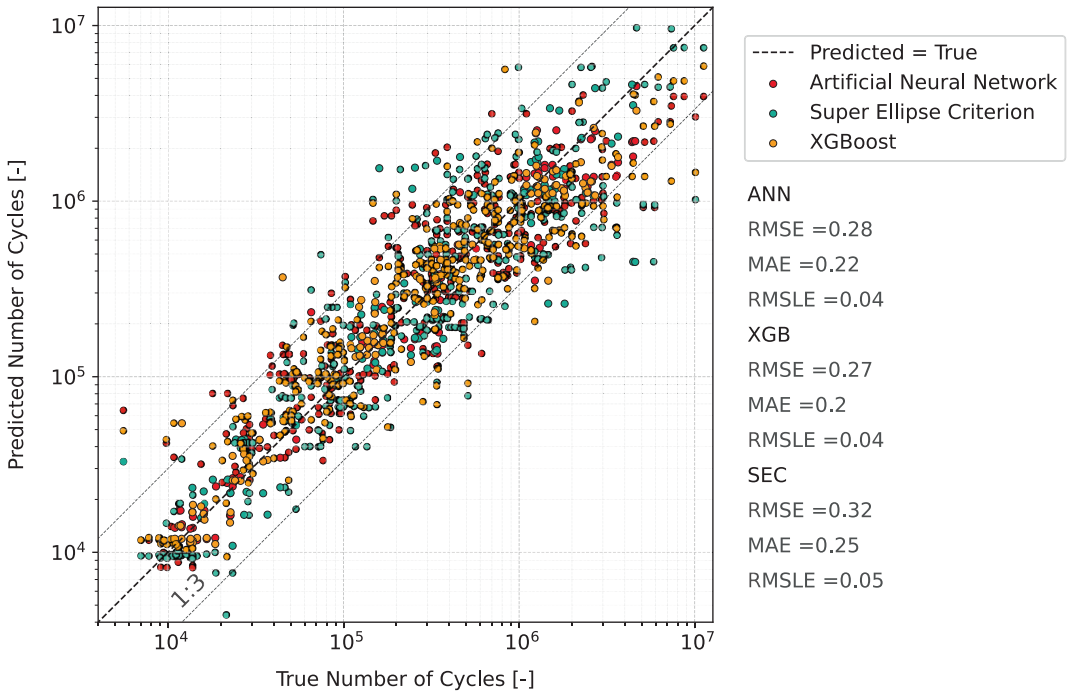

Fig. 13. All methods trained on the same features. The CV for XGB is carried out with random split.

generalizability. While the prediction of the ANN is independent of the type of data handling of the CV, the XGBoost model achieves high accuracy with random data splits and not with test program-wise data splits. This shows that the ANN learns the semi-elliptical relationship of the load parameters more independently of the data, which goes hand in hand with good generalizability to test programs not included in the training. The PDPs also show that the learned curves from the ANN are smoother and more stable than them of the XGBoost model. With the XGBoost models that were not trained on S-N curve parameters, it was shown that ML-based predictions are possible with satisfactory accuracy even without information about the associated S-N curves. It was shown that the greatest challenge lies in mapping more general influencing variables in the feature space of the models. Encoding categorical features, such as the weld condition and the base material, has a positive influence on the prediction. Other more general features such as the local weld geometry could further improve the prediction; however, any interpretation of the stress levels is based on nominal stresses, neglecting any stress rising effect of the weld toe or root notch. Considering stress gradient effects and thus including any geometric stress rising effects could lead to different findings. Moreover, there has been no evaluation of non-proportional loadings beyond phase shifts, dominant stress components, or multiaxial loading including stress components parallel to the weld. Although multiaxial loading with stresses parallel to the weld has been investigated in Bauer et al. [5], showing no difference between the assessment of different stress components. Moreover, the data including phase shifts lower than 90° is limited to very few test programs based on different materials. The derived effect of a 45° phase shift might therefore be coincidental. All findings are based on statistical correlations within the presented dataset. The generalizability of the results should be further examined as more data becomes available.

7. Conclusions

The comparison between the super ellipse criterion (SEC), an artificial neural network (ANN), and an extreme gradient boosting (XGBoost) machine learning (ML)model has confirmed that the ML-based models enable reliable prediction of fatigue life even with a limited database; however, there are differences between the ML methods due to the training algorithms. The following conclusions can be drawn from the comparison between the machine learning methods, their model-agnostic and model-specific interpretations, and the SEC approach:

- Overall, the ANN demonstrates superior performance, slightly outperforming the SEC in accuracy and the XGBoost model in terms of stability and generalizability across the available dataset.
- For the XGBoost model, the amount of data is too small to generalize to completely unknown test programs. This is shown by less accurate predictions when the 14-fold Cross Validation (CV) is program-wise and also by discontinuities in the Partial Dependence Plot (PDP).
- The XGBoost model provides very accurate predictions when trained on random data splits, where features that are not directly related to a test program, such as the base material or the post-treatment, can be used instead of the S-N curve parameters.
- The Shapley Additive Explanations (SHAP) analyses have shown that the normal stress and the shear stress have the greatest overall influence on the prediction, followed by the phase shift. This aligns with the findings derived from the PDP.
- When using categorical features such as the base material and the weld condition, these contribute significantly to the prediction with the XGBoost model.
- With the ANN, reliable predictions can be made regardless of the handling of the data for the CV, as the super-elliptical relationship of the stress components is learnt, which is reflected in smooth curves in the PDPs.

CRediT authorship contribution statement

Marten Beiler: Writing – original draft, Visualization, Methodology, Investigation, Data curation. **Niklas Michael Bauer:** Writing – original draft, Visualization, Validation, Software, Resources, Methodology, Investigation, Formal analysis, Data curation, Conceptualization. **Jörg Baumgartner:** Writing – review & editing, Supervision, Project administration, Funding acquisition. **Moritz Braun:** Writing – review & editing, Supervision, Project administration, Methodology, Funding acquisition, Conceptualization.

Declaration of competing interest

The authors declare that they have no known competing financial interests or personal relationships that could have appeared to influence the work reported in this paper.

Acknowledgement

The work was performed within the research project SMATRA – "Verbesserte Bewertung der Schwingfestigkeit geschweißter maritimer Tragstrukturen unter Anwendung lokaler Nachweiskonzepte" funded by the German Federal Ministry for Economic Affairs and Energy (project numbers 03SX559B and 03SX559C).

Data availability

Data will be made available on request.

References

[1] Pedersen MM. Multiaxial fatigue assessment of welded joints using the notch stress approach. Int J Fatigue 2016;83:269–79. https://doi.org/10.1016/j.ijfatigue.2015.10.021.
[2] Sonsino CM. Multiaxial fatigue of welded joints under in-phase and out-of-phase local strains and stresses. Int J Fatigue 1995;17:55–70. https://doi.org/10.1016/0142-1123(95)93051-3.
[3] Nakamura H, Takanashi M, Itoh T, Wu M, Shimizu Y. Fatigue crack initiation and growth behavior of Ti–6Al–4V under non-proportional multiaxial loading. Int J Fatigue 2011;33:842–8. https://doi.org/10.1016/j.ijfatigue.2010.12.013.
[4] Plank R, Kuhn G. Fatigue crack propagation under non-proportional mixed mode loading. Eng Fract Mech 1999;62:203–29. https://doi.org/10.1016/s0013-7944(98)00097-6.
[5] Bauer NM, Baumgartner J, Fass M. Fatigue life evaluation of welded joints under multiaxial loading for different stress concepts using an extended Gough-Pollard criterion. Weld World 2024. https://doi.org/10.1007/s40194-024-01716-6.
[6] Bäckström M, Marquis G. A review of multiaxial fatigue of weldments: experimental results, design code and critical plane approaches. Fatigue Fract Eng M 2001;24:279–91. https://doi.org/10.1046/j.1460-2695.2001.00284.x.
[7] R. Archer, Fatigue of a welded steel attachment under combined direct stress and shear stress. International conference of fatigue of welded constructions, no. paper; 1987.
[8] Hobbacher AF, Baumgartner J. Recommendations for Fatigue Design of Welded Joints and Components. 3rd ed. Cham, Switzerland: Springer International Publishing Switzerland; 2024.
[9] prEN 1993–1–9 – Eurocode 3: Design of Steel Structures – Part 1–9: Fatigue SC3 N3405 (unpublished); 2022.
[10] DNV-RP-C203: Recommended practice for Fatigue Design of offshore steel structures. Høvik, Norway; 2024.
[11] Analytical Strength Assessment of Components: FKM Guideline. VDMA, Frankfurt/Main; 2012.
[12] Sonsino CM. Multiaxial fatigue life response depending on proportionality grade between normal and shear strains/stresses and material ductility. Int J Fatigue 2020;135. https://doi.org/10.1016/j.ijfatigue.2019.105468.
[13] Bauer NM, Baumgartner J. Multiaxial fatigue life calculation of welded joints made of ductile materials. Weld World 2025. https://doi.org/10.1007/s40194-025-02080-9.
[14] Wächter RWM, Fällgren C, Beier H-T, Obermayr M, Rennert R, Vormwald M, et al. Multiaxial stresses in the FKM guideline - Status quo and how things could be improved. 14. International Conference on Multiaxial Fatigue and Fracture 2025. 2025.
[15] L'Heureux A, Grolinger K, Elyamany HF, Capretz MAM. Machine learning with big data: challenges and approaches. IEEE Access 2017;5:7776–97. https://doi.org/10.1109/access.2017.2696365.
[16] Murdock RJ, Kauwe SK, Wang A-Y-T, Sparks TD. Is Domain Knowledge Necessary for Machine Learning Materials Properties? Integrating Mater Manuf Innovation 2020;9:221–7. https://doi.org/10.1007/s40192-020-00179-z.
[17] Barbiero P, Squillero G, Tonda A. Modeling generalization in machine learning: A methodological and computational study. arXiv preprint arXiv:2006.15680; 2020.
[18] Yang JY, Kang GZ, Liu YJ, Kan QH. A novel method of multiaxial fatigue life prediction based on deep learning. Int J Fatigue 2021;151:106356. https://doi.org/10.1016/j.ijfatigue.2021.106356.
[19] Kalayci CB, Karagoz S, Karakas O. Soft computing methods for fatigue life estimation: a review of the current state and future trends. Fatigue Fract Eng M 2020;43:2763–85. https://doi.org/10.1111/ffe.13343.
[20] Awd MMM. Machine Learning Algorithm for Fatigue Fields in Additive Manufacturing. Wiesbaden: Springer Vieweg; 2022.
[21] Braun M, Kellner L. Comparison of machine learning and stress concentration factors-based fatigue failure prediction in small-scale butt-welded joints. Fatigue Fract Eng M 2022;45:3403–17. https://doi.org/10.1111/ffe.13800.
[22] Schubnell J, Aydogan Ö, Jung M. Determination of stress concentration factors of welded joints from 3D-surface scans by artificial neural networks. Procedia Struct Integrity 2024;57:112–20. https://doi.org/10.1016/j.prostr.2024.03.014.
[23] Schubnell J, Fliegener S, Rosenberger J, Feth S, Braun M, Beiler M, et al. Data-driven fatigue assessment of welded steel joints based on transfer learning. Weld World 2025;69:2223–38. https://doi.org/10.1007/s40194-025-01967-x.
[24] Zhang P, Tang K, Wang A, Wu H, Zhong Z. Neural network integrated with symbolic regression for multiaxial fatigue life prediction. Int J Fatigue 2024;188. https://doi.org/10.1016/j.ijfatigue.2024.108535.
[25] Nagode M, Papuga J, Oman S. Application of machine learning models for estimating the material parameters for multiaxial fatigue strength calculation. Fatigue Fract Eng M 2023;46:4142–60. https://doi.org/10.1111/ffe.14128.
[26] Choi D-K. Data-Driven Materials Modeling with XGBoost Algorithm and Statistical Inference Analysis for Prediction of Fatigue Strength of Steels. Int J Precis Eng Manuf 2019;20:129–38. https://doi.org/10.1007/s12541-019-00048-6.
[27] Beiler M, Tanvir M, Braun M. Weld Surface Geometry's Impact on Generalizability of Machine Learning Models for Fatigue Life Prediction. International Institute of Welding IIW-Doc. XIII-3071-2024; 2024.
[28] Wang X, Braun M. Explainable machine learning-based fatigue assessment of 316L stainless steel fabricated by laser-powder bed fusion. Int J Fatigue 2025;190. https://doi.org/10.1016/j.ijfatigue.2024.108588.
[29] Wang X, Braun M, Schubnell J. Ermüdungs- und Kerbwirkungsbewertung additiv gefertigter AISI 316L-Proben mittels physikalisch informierten maschinellen Lernverfahren. DVM-Arbeitskreis Arbeitskreis Additiv gefertigte Bauteile und Strukturen - Tagung 2025, Berlin, Germany; 2025.
[30] Kraus MA, Bartsch H. Discovery of fatigue strength models via feature engineering and automated eXplainable machine learning applied to the welded transverse stiffener. Int J Fatigue 2026;203. https://doi.org/10.1016/j.ijfatigue.2025.109324.
[31] Eibl M. Berechnung der Schwingfestigkeit laserstrahlgeschweißter Feinbleche mit lokalen Konzepten [PhD]. Darmstadt, Germany: Technische Universität Darmstadt; 2003.
[32] Exel N. Schwingfestigkeit laserstrahlgeschweißter Magnesiumknetlegierungen unter mehrachsigen proportionalen und nichtproportionalen Beanspruchungen. Shaker 2014.
[33] Bolchoun A. Eine Methode zur Festigkeitsbeurteilung von laserstrahlgeschweißten Magnesium-Verbindungen unter mehrachsigen Beanspruchungen mit konstanten und variablen Amplituden. Fraunhofer Verlag 2018.
[34] Bertini L, Cera A, Frendo F. Experimental investigation of the fatigue resistance of pipe-to-plate welded connections under bending, torsion and mixed mode loading. Int J Fatigue 2014;68:178–85. https://doi.org/10.1016/j.ijfatigue.2014.05.005.
[35] Frendo F, Bertini L. Fatigue resistance of pipe-to-plate welded joint under in-phase and out-of-phase combined bending and torsion. Int J Fatigue 2015;79:46–53. https://doi.org/10.1016/j.ijfatigue.2015.04.020.
[36] Razmjoo G. Fatigue of load-carrying fillet welded joints under multiaxial loading. In: 5 Th International Conference on Biaxial/Multiaxial Fatigue & Fracture; 1997. p. 53–70.
[37] Sonsino C. Schwingfestigkeit von geschweißten Komponenten unter komplexen elasto-plastischen, mehrachsigen Verformungen. 1018-5593; 1997.
[38] Sorsino C, Küppers M, Gäth N, Maddox SJ, Razmjoo GR. Fatigue behaviour of welded high-strength components under combined multiaxial variable amplitude loading; 1999.
[39] Störzel K, Wiebesiek J, Bruder T, Hanselka H. Betriebsfeste Bemessung von mehrachsig belasteten Laserstrahlschweißverbindungen aus Stahlfeinblechen des Karosseriebaus. LBF-Bericht Nr. FB-235, Darmstadt; 2008.
[40] Wiebesiek J. Festigkeitshypothesen zum Schwingfestigkeitsverhalten von dünnwandigen Laserstrahlschweißverbindungen aus Aluminium unter mehrachsigen Beanspruchungen mit konstanten und veränderlichen Hauptspannungsrichtungen. Shaker 2012.
[41] Winther NB, Jensen MA, Andreasen JH, Schjødt-Thomsen J, Larsen ML. Effect of non-proportional stress states caused by varying phase shifts on the fatigue life of welded joints. Int J Fatigue 2024;185. https://doi.org/10.1016/j.ijfatigue.2024.108351.
[42] Witt M. Schwingfestigkeit von Schweißverbindungen bei zusammengesetzter Betriebsbeanspruchung [Dissertation]. Technical University Clausthal 2000.
[43] Friedman JH. Greedy function approximation: A gradient boosting machine. The Annals of Statistics, 29; 2001: 1189–1232, 1144.
[44] Lundberg SM, Erion G, Chen H, DeGrave A, Prutkin JM, Nair B, et al. From local explanations to global understanding with explainable AI for trees. Nat Mach Intell 2020;2:56–67. https://doi.org/10.1038/s42256-019-0138-9.